Ceramics International (xxxx) xxxx–xxxx

Contents lists available at ScienceDirect

Ceramics International

journal homepage: www.elsevier.com/locate/ceramint

Effect of rotating speed during foaming procedure on the pore size distribution and property of silicon nitride foam prepared by using protein foaming method

Liuyan Yin*, Xingui Zhou, Jinshan Yu, Honglei Wang

Science and Technology on Advanced Ceramic Fibres & Composites Laboratory, National University of Defense Technology, Changsha 410073, China

ARTICLE INFO

Keywords:
B. Porosity
D. Si_3N_4
E. Functional applications

ABSTRACT

Silicon nitride (Si_3N_4) foams were prepared by using protein foaming method with varying rotating speed during the foaming process. The pore sizes of these as-fabricated Si_3N_4 foams were measured by means of the Image Pro Plus software and the as-measured pore size date was analyzed statistically by using the SPSS Statistics software. It was indicated that the pore size data of the as-prepared Si_3N_4 foams abided by the logarithmic normal distribution. With the increase of rotating speed, the pore structure of Si_3N_4 foam became more uniform. This was because of the enhancing shear stress at higher rotating speed, which increased frequency of collision between bubbles in foamed slurry and hence improved the uniformity of bubble size distribution. The porosity, density and flexural strength of these as-prepared Si_3N_4 foams fluctuated in a small range, indicating that the rotating speed had limited influence on these properties.

1. Introduction

Ceramic foam is a specific class of porous ceramic, which exhibits foam-like structure and high porosity. In ceramic foam, large numbers of spherical pores randomly and closely stack together. Owing to this typical structural feature, ceramic foam is widely used in various engineering applications, such as the high-temperature thermal insulation, support for catalytic, filtration of hot corrosive gases from diesel engine and artificial bone candidate [1–3]. Direct foaming method is one of the most commonly used methods in preparing ceramic foam. According the foaming way of this method, it can be classified as self-foaming route and air-incorporation foaming route. In the self-foaming route, the bubbles are formed by the released small molecules, which are derived from the pyrolysis of precursor [4–10] or the vaporization of the solvent [11]. While in the air-incorporation foaming route, the bubbles are formed by incorporating gas and stabilized by either particles, the surfaces of which are modified by short chain amphiphile molecules [12–16], or long chain surfactants which can be environmental friendly bio-molecules such as protein [17–20], starch [21–23] or a mixture of them [24,25]. When the protein is used as the foaming agent, this method can also be called as the protein foaming method. This method is derived from our daily life and it is economical and environmental friendly. The foaming mechanism of protein is attributed to the distribution of hydrophobic and hydrophilic regions within its primary structure [26–28], whereas the gelling mechanism of protein is due to its denature, similar to the boiling of egg.

Pore size distribution is a very important structure feature of ceramic foams and the investigation of the pore size distribution of ceramic foam is very fundamental and meaningful. Because an accurate pore structure model could be built and then many mechanical and functional properties could be simulated, once we know the pore size distribution of ceramic foams. Unfortunately, great efforts are still needed in this field, especially in finding the statistical rule of the pore size distribution of ceramic foams. To find this statistical rule of the pores size distribution, the processing parameters that have an influence on the pore size distribution of ceramic foams should be investigated firstly.

Similar to other air-incorporation foaming routes, the pores in the ceramic foams prepared by using the protein foaming method are mainly derived from the bubbles in the foamed slurry. As a result, the parameters, which have an influence on the size distribution of bubbles in the foamed slurry, also have an effect on the pore size distribution and property of the ceramic foam. Among them, the shear stress in foamed slurry during the foaming process, which is determined by the rotating speed, has a great influence on the size distribution of bubbles in wet foams, as we see in our daily life. However, it is scarce to find any researching paper, which investigates this aspect.

Unlike other kinds of porous materials, the mercury injection

* Corresponding author.
E-mail address: hanqing421720@sina.com (L. Yin).

http://dx.doi.org/10.1016/j.ceramint.2016.12.003
Received 23 November 2016; Received in revised form 28 November 2016; Accepted 1 December 2016

apparatus [23] or the nitrogen adsorption instrument are not suitable for charactering the pore size distribution of ceramic foam, especially for the ceramic foam with pores large than tens of micrometer. As an alternative, pore size distribution of ceramic foams can be characterized by X-ray tomography or via analyzing the SEM images of ceramic foams by certain software, for instance the Image Pro Plus. In this research, pore size distributions of Si_3N_4 foams prepared by using the protein foaming method with different rotating speed during the foaming process were investigated. Firstly, the sizes of pores in the as-prepared Si_3N_4 foams were measured by means of the Image Pro Plus software. Then, the obtained pore size data was statistically analyzed by using the SPSS Statistics software. It was indicated that the pore size values in the as-prepared Si_3N_4 foams abided by the logarithmic normal distribution. To the best of our knowledge, this is the first paper that reveals the statistical rule of the pore size distributions of ceramic foams prepared by using the protein foaming method.

2. Material and methods

2.1. Preparation of Si_3N_4 foam

Commercial Si_3N_4 powder (d_{50}=2.0 μm, purity of 99.9%, Beijing XinRongYuan Technology Co., Ltd) was dispersed into 120 ml distilled water by ball milling in a 500 ml bottle at a solid content of 34.7 vol%, together with 3 wt% Y_2O_3 and (purity of 99.99%, Sinopharm Chemical Reagent Co., Ltd) and 2 wt% Al_2O_3 (200–300 mesh, Sinopharm Chemical Reagent Co., Ltd). Morphology of the raw Si_3N_4 powder was shown in Fig. 1. Tetraamethylammonium hydroxide solution (TMAH, 25 wt%, Sinopharm Chemical Reagent Co., Ltd) was selected to adjust the pH value and the viscosity of Si_3N_4 slurry (4 ml TMAH solution for 120 ml distilled water). The mixture was ball-milled in a planetary mill (QM-3SP2, produced by Nanjin University, China) for about 20 h before adding 9 wt% (based on the weight of distilled water) egg albumen powder (protein content > 86.5%, Taiyo food (Tianjin) Co., Ltd). Two different sizes of zirconia balls (Ø 10 mm and Ø 8 mm) with a weight ratio of 1:1 were used. Total weight of the zirconia balls was controlled to be the same as the slurry. The suspension together with the egg albumen powder was rotated at different speed in the planetary ball milling for 45 min to foam the suspension.

After the foaming procedure, the foamed suspension was casted into a preservation box (LOCK & LOCK). Then the foamed suspension in the preservation box sealed by the cover was put in a water bath and consolidated at 80 °C for 2 h. Details about the consolidation procedure were also reported elsewhere [29,30]. After the consolidation procedure, the as generated green bodies were cooled to room temperature and then dried in air at room temperature. Then the protein was removed by burnout in air at the temperature of 500 °C for 1 h (In the temperature range of RT ~80 °C, the heating rate was 2 °C/min; in the temperature range of 80–150 °C, the heating rate was 0.5 °C/min; the temperature was held at 150 °C for 60 min; in the temperature range of 150–240 °C, the heating rate was 0.5 °C/min; in the temperature range of 240–500 °C, the heating rate was 0.3 °C/min; the temperature was held at 500 °C for 60 min; then the green bodies cooled with the furnace naturally.). Finally, the green bodies were sintered at the temperature of 1820 °C for 1.5 h under 0.3 MPa nitrogen pressure in a graphite furnace (High-multi 5000, Japan) with a heating rate of 5 °C/min above 1000 °C. During the cooling process, the cooling rate was controlled to be 10 °C/min above 1200 °C. Powder bed consisted of 50 wt% BN powder and 50 wt% Si_3N_4 powder was used during the sintering of Si_3N_4 foams.

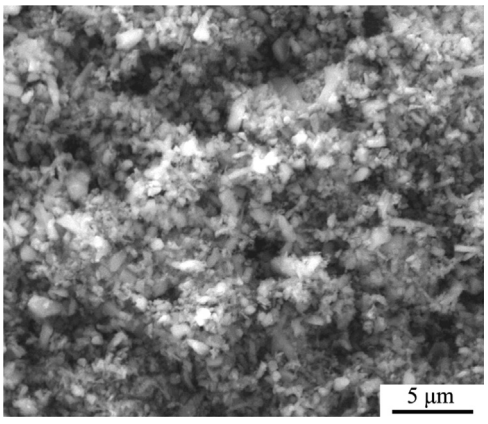

Fig. 1. Morphology of the raw Si_3N_4 powder.

2.2. Characterization of Si_3N_4 foam

Powder X-ray diffraction (XRD) patterns of the as-received Si_3N_4 powder and the sintered Si_3N_4 foam were determined by means of an X-ray diffractometer (D8 Advance, Bruker, Germany) at 40 kV and 40 mA, with a Cu Kα2 radiation source.

The density and open porosity of the Si_3N_4 foams were measured by using the Archimedes method. Total porosity of the Si_3N_4 foams was calculated according to the ratio between the measured density of Si_3N_4 foam and the theoretical density of the sintered Si_3N_4. Flexural strength of the Si_3N_4 foams was measured by universal testing machine (WDW-100, China) with a crosshead speed of 0.5 mm/min. The size of the Si_3N_4 foam for flexural strength measurement was 3×4×45 mm^3. The span of Si_3N_4foams for flexural strength measurement was 30 mm. At least five specimens were used to determine the average flexural strength. Pore structure was characterized by scanning electron microscopy (FEI Quanta-200 ESEM, USA). Average pore size was obtained by analyzing SEM images of Si_3N_4 foams by means of the Image-Pro Plus 6.0 software [30]. In this software, the pores were outlined manually and then the average diameter of every pore was calculated by this software automatically. All the pores in two SEM images (magnify at 50 times) of every Si_3N_4 foam were chosen. Then the data of these obtained pore size was statistically analyzed by the SPSS Statistics 17.0 software.

3. Results

Typical powder XRD patterns of the raw Si_3N_4 powder and the Si_3N_4 foam sintered at 1820 °C are shown in Fig. 2. As shown in Fig. 2, there are both α-Si_3N_4 phase and β-Si_3N_4 phase in the raw Si_3N_4 powder. The percentage of α-Si_3N_4 phase in the raw Si_3N_4 powder was calculated to be 87.1% according to the XRD pattern by using the

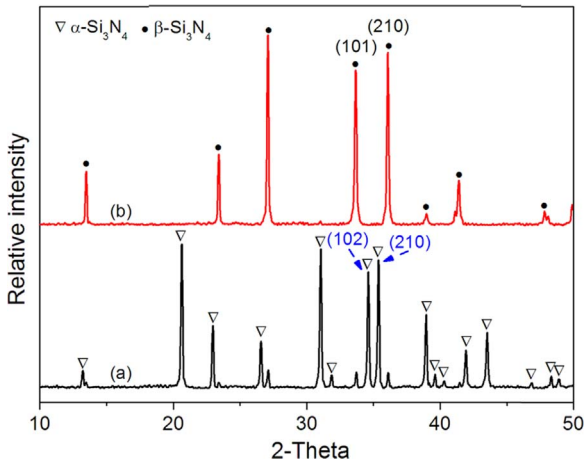

Fig. 2. Powder XRD patterns of the raw Si_3N_4 powder (a) and the Si_3N_4 foam at 1820 °C (b).